Melanopsin Phototransduction Contributes to Light-Evoked Choroidal Expansion and Rod L-Type Calcium Channel Function In Vivo

Bruce A. Berkowitz,[1,2] Tiffany Schmidt,[3] Robert H. Podolsky,[4] and Robin Roberts[1]

[1]Department of Anatomy and Cell Biology, Wayne State University, Detroit, Michigan, United States
[2]Department of Ophthalmology, Wayne State University, Detroit, Michigan, United States
[3]Department of Neurobiology, Northwestern University, Evanston, Illinois, United States
[4]Department of Family Medicine and Public Health Sciences, Wayne State University, Detroit, Michigan, United States

Correspondence: Bruce A. Berkowitz, Department of Anatomy and Cell Biology, Wayne State University School of Medicine, 540 E. Canfield, Detroit, MI 48201, USA; baberko@med.wayne.edu.

Submitted: June 23, 2016
Accepted: August 25, 2016

Citation: Berkowitz BA, Schmidt T, Podolsky RH, Roberts R. Melanopsin phototransduction contributes to light-evoked choroidal expansion and rod l-type calcium channel function in vivo. *Invest Ophthalmol Vis Sci*. 2016;57:5314–5319. DOI:10.1167/iovs.16-20186

Purpose. In humans, rodents, and pigeons, the dark → light transition signals nonretinal brain tissue to increase choroidal thickness, a major control element of choroidal blood flow, and thus of photoreceptor and retinal pigment epithelium function. However, it is unclear which photopigments in the retina relay the light signal to the brain. Here, we test the hypothesis that melanopsin (*Opn4*)-regulated phototransduction modulates light-evoked choroidal thickness expansion in mice.

Methods. Two-month-old C57Bl/6 wild-type (B6), 4- to 5-month-old C57Bl/6/129S6 wild-type (B6 + S6), and 2-month-old melanopsin knockout ($Opn4^{-/-}$) on a B6 + S6 background were studied. Retinal anatomy was evaluated in vivo by optical coherence tomography and MRI. Choroidal thickness in dark and light were measured by diffusion-weighted MRI. Rod cell L-type calcium channel (LTCC) function in dark and light (manganese-enhanced MRI [MEMRI]) was also measured.

Results. $Opn4^{-/-}$ mice did not show the light-evoked expansion of choroidal thickness observed in B6 and B6 + S6 controls. Additionally, $Opn4^{-/-}$ mice had lower than normal rod cell and inner retinal LTCC function in the dark but not in the light. These deficits were not due to structural abnormalities because retinal laminar architecture and thickness, and choroidal thickness in the $Opn4^{-/-}$ mice were similar to controls.

Conclusions. First time evidence is provided that melanopsin phototransduction contributes to dark → light control of murine choroidal thickness. The data also highlight a contribution in vivo of melanopsin phototransduction to rod cell and inner retinal depolarization in the dark.

Keywords: MRI, retina, diffusion, choroidal thickness, rod cells, L-type calcium channels

Choroidal blood flow is essential for maintaining healthy rods, cones, and retinal pigment epithelium (RPE) in the posterior segment. Studies in human, rat, and pigeon have established that choroidal thickness, an important regulator of choroidal blood flow, is controlled largely by nonretinal brain tissue via autonomic innervation.[1–10] There are, however, gaps in our understanding of this neuronal regulation of choroidal thickness. For example, while the autonomic system certainly does not generally require input from the retina to function, brain-modulated choroidal thickness has a curious and well-established light-dependence.[1,7–14] Because this effect is light dependent, the retina is required to mediate it. The initiating retinal photopigment(s) remain unidentified. One possibility involves melanopsin (*Opn4*), the photopigment responsible for direct light-sensing in intrinsically photosensitive retinal ganglion cells (ipRGC). These cells represent plausible candidates for this influence because they project to brain regions, such as the paraventricular nucleus of the hypothalamus (PVN), which innervates to both the choroid and ipRGCs.[12,13,15] The PVN also receives input from the suprachiasmatic nuclei (SCN), another ipRGC target.[15,16]

One hurdle to addressing the above question is that conventional methods, such as optical coherence tomography (OCT), cannot study in vivo choroidal thickness in complete darkness. In this study, we address this problem by using diffusion-weighted MRI to measure in vivo the dark → light expansion of choroidal thickness in mice.[4,17] To examine if melanopsin contributes to other aspects of retinal physiology not necessarily related to the choroidal changes, a secondary goal of this study was to examine in vivo possible functional consequences of lack of melanopsin phototransduction on L-type calcium channels (LTCCs) in different cell layers as measured by manganese-enhanced MRI (MEMRI).[18] Manganese-enhanced MRI is the method of choice for analytically evaluating LTCC function from awake and freely moving animals. For example, dark adaptation normally causes rod cell membranes to depolarize resulting in opening of LTCCs with increased manganese uptake compared with that in the light when rod cell membranes are normally hyperpolarized and LTCCs are closed.[18–22] In this paper, we show that melanopsin phototransduction is required for both normal choroidal

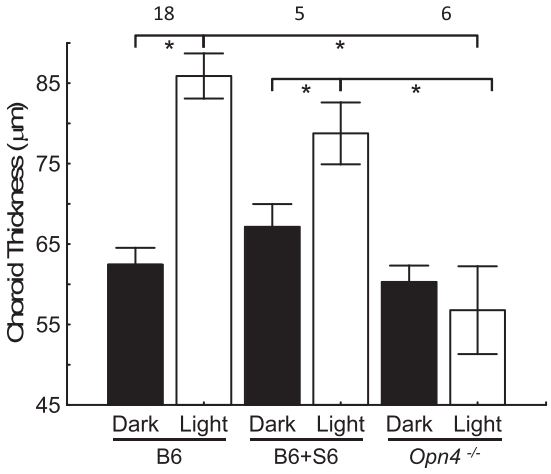

Figure 1. Summary of objectively determined dark (*black bar*) and 20 minutes of approximately 500-lux light (*white bar*) choroidal thicknesses measured from in B6, B6 + S6, and *Opn4*$^{-/-}$ mice. *Significant difference ($P < 0.05$) indicated by *brackets. Error bars*: SEM.

expansion during the dark → light transition as well as normal dark-adapted LTCC function in vivo.

Methods

All animals were treated in accordance with the National Institutes of Health Guide for the Care and Use of Laboratory Animals, the ARVO Statement for the Use of Animals in Ophthalmic and Vision Research, and Institutional Animal and Care Use Committee authorization. Animals were housed and maintained in 12 hour:12 hour light-dark cycle laboratory lighting, unless otherwise noted.

Groups

The following groups were studied between 9 AM and 3 PM: 2-month-old C57Bl/6 wild-type (B6; Jackson Laboratories, Bar Harbor, ME, USA), 4- to 5-month-old C57Bl/6/129S6 wild-type (B6 + S6), and 2-month-old melanopsin knockout (*Opn4*$^{-/-}$) on a B6 + S6 background (a kind gift from David Berson, PhD; Brown University, Providence, RI, USA).

Optical Coherence Tomography

To compare retinal laminar anatomy, and help calibrate the spatial location of transretinal MRI information, subsets of mice from each group ($n = 2$) were anesthetized with urethane (36% solution intraperitoneally; 0.083 mL/20 g animal weight, prepared fresh daily; Sigma-Aldrich Corp., St. Louis, MO, USA) and examined using OCT (Envisu R2200 VHR SDOIS; Bioptigen, Inc., Morrisville, NC, USA).

Magnetic Resonance Imaging

The general mouse preparation for high resolution MRI is well established in our laboratory.[23] All animals were maintained in darkness for at least 16 hours before and during the dark-phase of the MRI examination. Mouse groups were either untreated, or treated with $MnCl_2$ either under dim red light (dark) or after 20 minutes of light exposure as an intraperitoneal injection (66 mg $MnCl_2$•4 H_2O/kg) on the right side of awake mice.[24,25] After this injection, mice were maintained in the dark (or light) for another 3.5 to 4 hours. High-resolution anatomic and apparent diffusion coefficient (ADC) data were acquired in the untreated mice on a 7 T system (Bruker ClinScan, Billerica, MA, USA) using a receive-only surface coil (1.0-cm diameter) centered on the left eye. The end of a fiber optic bundle was attached to a light source (Mark II Light Source; Prescott's, Inc., Monument, CO, USA) placed caudal to the eye, projecting at a white screen approximately 1 cm from eye, similar to that previously described.[17] We exposed the eye to 0 (i.e., dark) or approximately 500 lux (confirmed outside the magnet using a Traceable Dual-Range Light Meter [Control Company, Friendswood, TX, USA]) placed against a 1-cm diameter aperture; measured this way, room lighting is approximately 300 lux). Aside from the fiber optic light source, all lights in the MRI room were turned off. In all groups, immediately before the MRI experiment, animals were anesthetized with urethane (36% solution intraperitoneally; 0.083 mL/20 g animal weight, prepared fresh daily; Sigma-Aldrich Corp.) and treated topically with 1% atropine to ensure dilation of the iris during light exposure followed by 3.5% depth lidocaine gel to reduce sensation that might trigger eye motion, and to keep the ocular surface moist. Apparent diffusion coefficient MRI data were collected parallel to the optic nerve, the most sensitive direction for detecting changes in the extracellular space around the outer segments.[17] Apparent diffusion coefficient MRI data sets were collected, first in the dark and then again 15 minutes after turning on the light; because each ADC data set takes 10 minutes to collect, we refer to the midpoint in the ADC collection as 20 minutes of light exposure. Anatomic images were acquired using a spin-echo sequence (slice thickness 600 μm, repetition time [TR] 1000 ms, echo time [TE] 11 ms, matrix size 192 × 320, field of view 8 × 8 mm^2, NA 2, axial resolution for central retina 25 μm). Images sensitized to water diffusion were collected (TR 1000 ms, slice thickness 600 μm, TE 33 ms, matrix size 174 × 288, field of view 8 × 8 mm^2, axial resolution for central retina 27.8 μm; b = 0, 100, 250, 500, 600, 750, 990 s/mm^2 [collected in pseudorandom order, number of acquisitions (NA) = 1 per b-value (b-value is the variable that changes the degree of diffusion weighting)]), registered to the anatomic image, and analyzed (using in-house code) to generate ADC profiles from the central retina.

Manganese-enhanced MRI data were acquired using several single spin-echo acquisitions (time to echo 13 ms, 7 × 7 mm^2, matrix size 160 × 320, slice thickness 600 μm). Images were acquired at different TRs in the following order (number per time between repetitions in parentheses): TR 0.15 seconds,[6] 3.50 seconds,[1] 1.00 seconds,[2] 1.90 seconds,[1] 0.35 seconds,[4] 2.70 seconds,[1] 0.25 seconds,[5] and 0.50 seconds.[3] To compensate for reduced signal-noise ratios at shorter TRs, progressively more images were collected as the TR decreased. B6 data in Figures 1 and 2 have been previously presented elsewhere.[4,25]

The present resolution in the central retina is sufficient for extracting meaningful layer-specific anatomic and functional data, as previously discussed.[4,25] In all cases, animals were humanely euthanized as detailed in our Division of Laboratory Animal Resources (DLAR)-approved protocol.

Data Analysis

In each animal, we confirmed ocular dilation based on the iris position on the anatomic MRI data; if eyelid position was closed to a degree likely to impede the light path, only the dark data from that animal was used.[26] All images for each animal per lighting condition were registered (rigid body) to the anatomic image and ADC calculated, as previously described.[26] In all cases, the same central retinal regions-of-interest (±0.4–1 mm from the optic nerve head) were analyzed; thickness, ADC, and manganese uptake values from the superior and inferior retina were respectively averaged. A figure illustrating how the

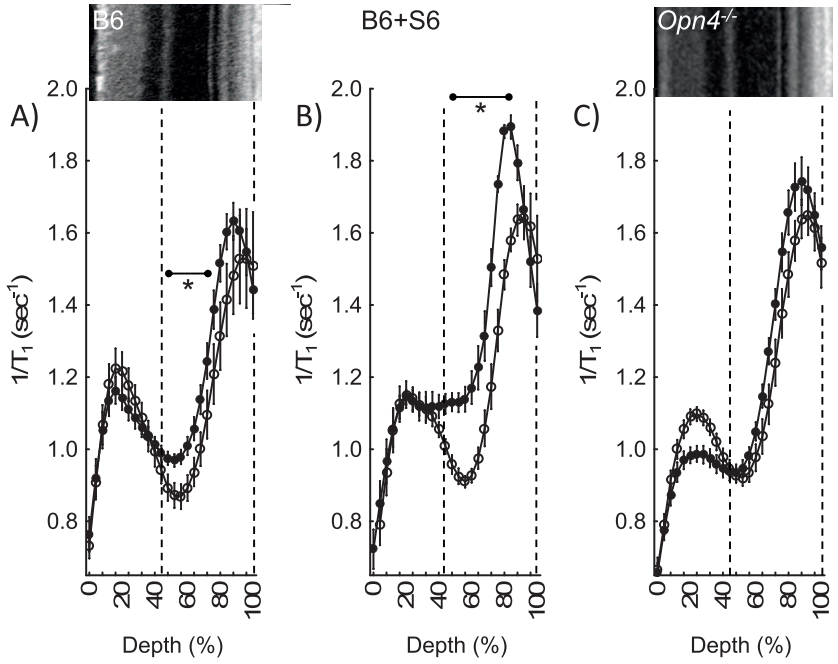

Figure 2. Summary of central retinal MEMRI as a function of retinal depth during dark (*closed black symbols*) and light adapted (*open symbols*) conditions in (**A**) B6 ($n = 19$, dark; $n = 11$, light), (**B**) B6 + S6 ($n = 7$, dark; $n = 5$, light), and (**C**) *Opn4*$^{-/-}$ ($n = 15$, dark; $n = 12$, light) mice; details are in the Supplementary Table. Approximate location of two anatomical landmarks are indicated by dotted lines (i.e., anterior aspect of the outer plexiform layer [*left*] and retina/choroid border [*right*]). Profiles are spatially normalized to dark adapted retinal thickness (0% = vitreous/retina border, 100% = retina/choroid border). *Retinal depth range with significant difference. *Error bars*: SEM.

choroid thickness was performed from diffusion-weighted MRI data is presented elsewhere.[4]

In each mouse, thicknesses (μm) from the anatomic and ADC images were objectively determined using the "half-height method," wherein a border is determined via a computer algorithm based on the crossing point at the midpoint between the local minimum and maximum, as detailed elsewhere.[26,27] The distance between two neighboring crossing-points, thus represents an objectively defined thickness.

From the anatomic image, thicknesses were normalized with 0% depth at the presumptive vitreoretinal border and 100% depth at the presumptive retina–choroid border. Note that because of partial volume averaging there are slight contributions from nonretinal tissue anteriorly at the vitreo-retinal border and posteriorly at the retina–choroid border.

Accurate estimates of choroidal thickness (defined as a combination of the choroid and choriocapillaris) in each mouse compared with published values obtained using other methods are feasible using diffusion weighted MRI.[4,25] We take advantage of the fact that ADC images show a suppressed signal from the vertical vessels between the horizontal segments of the choroid and the choroidal capillaries (i.e., the direction parallel to the optic nerve) and the vitreous (which has higher ADC than retina due to the lack of cellular barriers[28]). We then used the same computer algorithm as above to objectively determine the thickness from the portion of retina that was not suppressed in the averaged (to improve signal-to-noise) b100-b990 diffusion images; herein this is referred to as the ADC thickness. The thickness difference between that generated from the anatomic image (e.g., with a choroid contribution), and that generated from the ADC image (with suppressed choroidal contribution), was considered an estimate of the choroid thickness for each mouse. In this manner, choroidal thicknesses were estimated for dark and light exposed conditions for each mouse; the accuracy of this choroidal thickness estimate has been confirmed in several models.[4,25]

As per our earlier studies, the ADC profiles in dark and light in each mouse were spatially normalized to the anatomical thickness value in the dark (because our data indicated that the "extra" thickness in the light was primarily via expansion of the choroid in the light).

Evaluations of choroid and extracellular space around the outer segments (OS) were done objectively, based strictly on dark adapted anatomic thickness values (as described above), and thus data were not masked.

Manganese-enhanced MRI data from the central retinal were analyzed as previously described.[4,25] Single images acquired with the same TR were first registered (rigid body) and then averaged. These averaged images were then registered across TRs. The same regions-of-interest as above were analyzed by calculating 1/T1 maps by first fitting to a three-parameter T1 equation ($y = a + b * [\exp(-c*TR)]$, where a, b, and c are fitted parameters) on a pixel-by-pixel basis using R (v.2.9.0; R Development Core Team [2009], R: A language and environment for statistical computing. R Foundation for Statistical Computing, Vienna, Austria. ISBN: 3-900051-07-0) scripts developed in-house, and the minpack.lm package (v.1.1.1; Timur V. Elzhov and Katharine M. Mullen, minpack.lm: R interface to the Levenberg-Marquardt nonlinear least-squares algorithm found in MINPACK. R package version 1.1–1). The reciprocal (1/T1) values are proportional to manganese levels. Central intraretinal 1/T1 profiles were obtained as detailed elsewhere.[26] Values from the superior and inferior retina were averaged. Note that only those animals that took up manganese above baseline (i.e., ~0.65 s^{-1}) were included in the final analysis.

Statistical Analysis

All thicknesses in each group were evaluated for a normal distribution and were compared using a one-way ANOVA test;

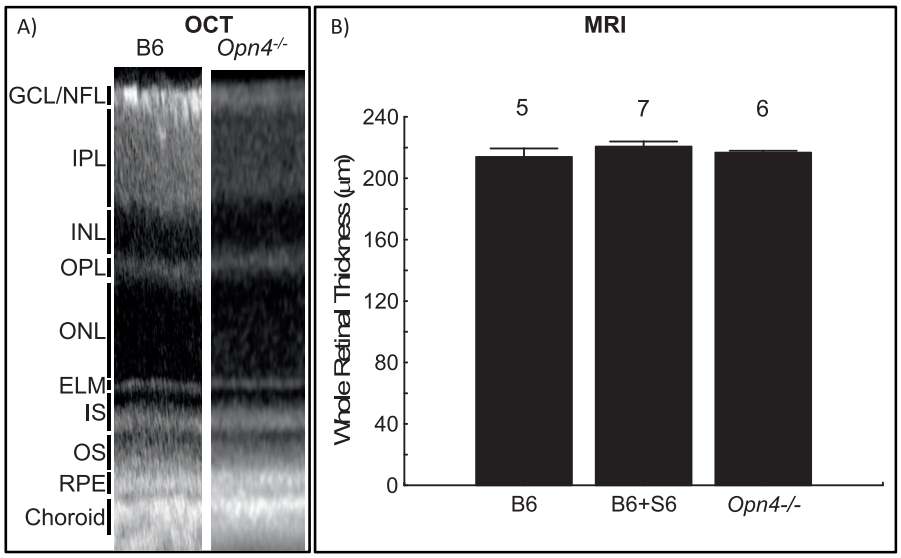

Figure 3. Summary of retinal anatomy for each group from (**A**) representative OCT data and (**B**) group MRI data (numbers above bars = number of animals; *Error bars*: SEM). We were unable to obtain OCT from B6 + S6 mice but given the similar laminar structure and whole retinal thickness between B6 and *Opn4*$^{-/-}$ mice, we assume laminar structure is similar between B6 and B6 + S6 mice. RGC/NFL, retinal ganglion cell layer / nerve fiber layer; IPL, inner plexiform layer; INL, inner nuclear layer; OPL, outer plexiform layer; ONL, outer nuclear layer; ELM, external limiting membrane; IS, inner segments of rod cells (ellipsoid region); OS, outer segments of rod cells; RPE, retinal pigment epithelium.

negative results are presented with 95% confidence intervals (CI). In some animals, eyelids were not open sufficiently, preventing collection of both dark and light data from all animals. Data are presented as mean ± SEM. We used generalized estimating equations (GEE) to examine differences in MEMRI between the dark and light groups. This approach appropriately accounts for the correlation among neighboring pixel values within animals. We used a first-order autoregressive correlation structure, with similar results obtained using an unstructured correlation matrix. We preselected location ranges strictly based on the distance between retinal layers as measured by OCT: 0% to 24% depth representing retinal ganglion cell (RGC) and inner plexiform layer (IPL); 28% to 40%, the inner nuclear layer (INL); 48% to 72%, the outer nuclear layer (ONL); 76% to 84%, the inner segment (IS) region of the rod cells; and 88% to 100%, the OS region of the rod cell and RPE. To control for multiple testing across the regions, we used the Holm correction to adjust the GEE-generated *P* values from each location range. Although the false discovery rate was considered, this method could not be used due to the relatively small number of tests and lack of independence across the location regions. Further, the sample sizes we used would result in low comparison-wise power. As such, we used an overall type 1 error rate of 0.1.

Results

Effect of Dark and Light on Choroidal Thicknesses

To determine whether melanopsin phototransduction was required for changes in choroidal thickness during dark → light transition, we measured choroidal thickness in vivo using diffusion-weighted MRI. *Opn4*$^{-/-}$ mice did not show a light-evoked increase in choroidal thickness (–6 ± 9%, $n = 6$) and their choroidal thickness in the light was lower ($P < 0.05$) than that in B6 + S6 controls (Fig. 1). This is in contrast to the significant ($P < 0.05$) light-dependent expansion of the choroidal thickness observed in the B6 (39 ± 7%, mean ± SEM, $n = 17$) and B6 + S6 (18 ± 5%, $n = 5$) wild-type groups (Fig. 1). Also, control groups from both backgrounds (B6 and B6 + S6) showed no difference in choroidal thickness in the light (86 ± 3 µm vs. 79 ± 4 µm, respectively, $P > 0.05$). Importantly, choroidal thickness in the dark in vivo was not different between *Opn4*$^{-/-}$ mice and controls indicating that choroidal function but not anatomy is different between experimental and controls (Fig. 1). These data indicate that melanopsin phototransduction is required for light-evoked influences on choroidal thickness.

Manganese-Enhanced MRI

To date, a contribution of the melanopsin phototransduction pathway to rod cell membrane polarization in dark and light has not been investigated. *Opn4*$^{-/-}$ mice did not show significant uptake differences in dark and light (Fig. 2C). In contrast, dark adapted B6 control mice (with rod cell membrane depolarization and LTCCs opening) increases manganese uptake in rod cells nuclei (48%–72% depth) compared with that in the light when rod cell membrane are normally hyperpolarized and LTCCs are closed (Fig. 2A).[19–22] B6 + S6 control mice showed a more spatially extensive pattern of greater rod cell uptake of manganese in the dark than in the light (48%–84% depth, Fig. 2B).

Retinal Anatomy

The distance between retinal layers on OCT appeared similar on visual inspection between *Opn4*$^{-/-}$ mice and B6 controls (Fig. 3). Similarly, quantification revealed no significant differences in whole retinal thicknesses between groups as measured by MRI *Opn4*$^{-/-}$ mice (95% CI [214, 220 µm]; B6 [198, 229 µm]; B6 + S6 [212, 229 µm]; Fig. 3).

Discussion

In this study, we present evidence that melanopsin contributes to light-evoked expansion of the choroid in the mouse. Given the substantial literature in human, rat, and pigeon, it seems reasonable to assume that the choroidal thickening observed in the mouse in the dark/light transition was under nonretinal

neuronal control but that assumption was not tested herein.[4] The other major observation in this study (not necessarily related to choroidal thickness changes with light) was that dark adapted *Opn4*$^{-/-}$ mice had subnormal manganese uptake in inner and outer retina, consistent with inappropriate hyperpolarization of several different cell types including rod cells in the dark. Previously, we demonstrated that the cell layer containing ipRGCs in postnatal day 7 *Opn4*$^{-/-}$ mice (when the density of melanopsin-containing RGCs is higher than in adults, and rod and cone inputs are absent) exhibited a low uptake of manganese in the light consistent with a hyperpolarized membrane in contrast to its normal depolarization in the light in controls.[20] This suggests that cells that are normally depolarized in the dark, such as rod cells, depend to some extent on the presence of melanopsin. More work is now needed to investigate the underlying mechanisms of the present findings.

Though we did not directly test for the role of dopamine in choroidal expansion, previous findings have suggested that light-evoked release of dopamine by amacrine cells can transiently increase choroidal thickness.[29] The role of dopamine in light-activated choroidal expansion was not the focus of this study. However, the present MEMRI data may indirectly test for a role of light-dependent release of dopamine in choroidal expansion. Light is a robust regulator of dopamine release by amacrine cells, and dopamine inhibits membrane polarization in, for example, rod cells in bright light. No significant changes in the transretinal MEMRI profiles in the light were observed in the *Opn4*$^{-/-}$ mouse raising the possibility that light-dependent dopamine signaling is not altered by the absence of melanopsin, and thus that dopamine signaling not likely a contributor to lack of choroidal thickness change in the dark/light transition observed in the melanopsin knockout mouse. However, more work needs to be done in the future to directly to rule out the role of dopamine in this process.

There are few studies available for comparison of the present results. In 2013, Shih et al.[10] found little evidence for a light driven increases in ChBF in rats using microspheres. There are several potentially important differences between our study and that of Shih et al.:[10] (1) species used (mouse [present study] versus rat[10]), (2) pigment (present study) versus nonpigment,[10] (3) duration of dark adaptation (overnight [present study] versus 30 minutes[10]), (4) duration of light exposure (20 minutes (present study) vs. 30 minutes[10]), and (5) light intensity (physiologic [~550 lux, present study] versus nonphysiologic [17,500 lux][10]). Also, it is unclear under what conditions microspheres can detect the roughly 10- to 20-μm light-evoked change in choroidal thickness measured in the present study. Future experiments that examine each factor are justified but are not the focus of the present study.

One potential confounder in this study is that choroidal thickness does decrease with age.[30,31] However, the present range of mouse ages falls within a mature mouse range and would not be expected to display an "aging" phenotype. For example, the neuroscience information framework (NIF) has defined (NIF Annotation Standards for Age Classification) a mature mouse as 3- to 6-months old (day of birth = day 0), a middle adult mouse as 10- to 14-months old, and an old mouse as 18-months to 2-years old. In a preliminary study, we find no differences in choroidal thickness in the dark between mature and middle adult B6 (10 months) mice (95% CI [58, 67 μm] dark mature B6, 95% CI [38, 73 μm] dark middle age B6). In addition, our key outcome measure, the increase in choroidal thickness between dark and light, is significant ($P < 0.05$) in both mature and middle adult B6 groups but not different between them (95% CI [26%, 53%] mature B6; [4%, 33%] middle adult B6). Thus, the age range of the mice in this study does not seem likely to generate a meaningful change in choroidal thickness.

A major limitation of the present study is that the melanopsin-containing cell-type was not identified. One possibility, given the substantial posterior segment LTCC abnormalities we find in the absence of melanopsin, is that the present findings are a result of melanopsin phototransduction in, for example, the RPE. Intriguingly, a couple of studies have reported melanopsin in RPE.[32,33] However, those studies find the level of RPE melanopsin is quite low and thus its functional importance remains unclear.[32,33] In fact, our functional MEMRI studies did not show significant changes between dark versus light RPE membrane polarization between wild-type or *Opn4*$^{-/-}$ mice (Fig. 2).[20] It is possible that the light-stimulated expansion of the choroid is due to rod cells (the dominant outer retinal photoreceptor in mice[34]). However, our previous work demonstrated that mice deficient in rod phototransduction (transducin alpha knockout; *Gnat1*$^{-/-}$ mice) show normal choroidal thickness and normal light-induced choroidal expansion[4] despite having decreased LTCC function in the dark.[25] Thus, rod function does not appear to be required for light-dependent choroidal expansion. On the other hand, functional melanopsin is established to be located in ipRGCs,[16,33] and choroid and ipRGC both have innervation to, for example, the paraventricular hypothalamus.[12,13,15,35,36] Taken together, the above considerations raise the possibility that melanopsin-containing ipRGC's control light-activated choroidal expansion, but more work is needed to test this hypothesis.

In conclusion, we find first time evidence that melanopsin contributes to expansion of murine choroidal thickness in the transition from dark to light. These data are consistent with nonretinal neuronal control of choroidal thickness. Also, our functional MEMRI data raise the possibility that melanopsin phototransduction regulates a signal that promotes inner retinal cells and rod cell depolarization in the dark. More work is needed to identify the nature of this signal.

Acknowledgments

The authors thank David Berson, PhD, (Brown University, Providence, RI, USA) for his useful suggestions throughout this study and for comments on a preliminary draft of this manuscript.

Supported by the National Eye Institute (R21 EY021619, BAB; RO1 EY026584; Bethesda, MD, USA), an unrestricted grant from Research to Prevent Blindness (Kresge Eye Institute; New York, NY, USA), and Northwestern University's Searle Leadership Fund in the Life Sciences (TS; Evanston, IL, USA).

Disclosure: **B.A. Berkowitz**, None; **T. Schmidt**, None; **R.H. Podolsky**, None; **R. Roberts**, None

References

1. Nickla DL, Wallman J. The multifunctional choroid. *Prog Retin Eye Res*. 2010;29:144–168.
2. Fuchsjäger-Mayrl G, Polska E, Malec M, Schmetterer L. Unilateral light-dark transitions affect choroidal blood flow in both eyes. *Vision Res*. 2001;41:2919–2924.
3. Longo A, Geiser M, Riva CE. Subfoveal choroidal blood flow in response to light-dark exposure. *Invest Ophthalmol Vis Sci*. 2000;41:2678–2683.
4. Berkowitz BA, Grady EM, Khetarpal N, Patel A, Roberts R. Oxidative stress and light-evoked responses of the posterior segment in a mouse model of diabetic retinopathy. *Invest Ophthalmol Vis Sci*. 2015;56:606–615.
5. Zhao M, Yang XF, Jiao X, et al. The diurnal variation pattern of choroidal thickness in macular region of young healthy female

individuals using spectral domain optical coherence tomography. *Int J Ophthalmol*. 2016;9:561–566.

6. Iwase T, Yamamoto K, Ra E, Murotani K, Matsui S, Terasaki H. Diurnal variations in blood flow at optic nerve head and choroid in healthy eyes: diurnal variations in blood flow. *Medicine*. 2015;94:e519.
7. Brown JS, Flitcroft DI, Ying GS, et al. In vivo human choroidal thickness measurements: evidence for diurnal fluctuations. *Invest Ophthalmol Vis Sci*. 2009;50:5–12.
8. Nickla DL, Wildsoet CF, Troilo D. Diurnal rhythms in intraocular pressure axial length, and choroidal thickness in a primate model of eye growth, the common marmoset. *Invest Ophthalmol Vis Sci*. 2002;43:2519–2528.
9. Papastergiou GI, Schmid GF, Riva CE, Mendel MJ, Stone RA, Laties AM. Ocular axial length and choroidal thickness in newly hatched chicks and one-year-old chickens fluctuate in a diurnal pattern that is influenced by visual experience and intraocular pressure changes. *Exp Eye Res*. 1998;66:195–205.
10. Shih YY, Wang L, De La Garza BH, et al. Quantitative retinal and choroidal blood flow during light dark adaptation and flicker light stimulation in rats using fluorescent microspheres. *Curr Eye Res*. 2013;38:292–298.
11. Fitzgerald ME, Gamlin PD, Zagvazdin Y, Reiner A. Central neural circuits for the light-mediated reflexive control of choroidal blood flow in the pigeon eye: a laser Doppler study. *Vis Neurosci*. 1996;13:655–669.
12. Li C, Fitzgerald MEC, LeDoux MS, et al. Projections from the hypothalamic paraventricular nucleus and the nucleus of the solitary tract to prechoroidal neurons in the superior salivatory nucleus: pathways controlling rodent choroidal blood flow. *Brain Res*. 2010;1358:123–139.
13. Fuchsjäger-Mayrl G, Malec M, Amoako-Mensah T, Kolodjaschna J, Schmetterer L. Changes in choroidal blood flow during light/dark transitions are not altered by atropine or propranolol in healthy subjects. *Vision Res*. 2003;43:2185–2190.
14. Kur J, Newman EA, Chan-Ling T. Cellular and physiological mechanisms underlying blood flow regulation in the retina and choroid in health and disease. *Prog Retin Eye Res*. 2012;31:377–406.
15. Hattar S, Kumar M, Park A, et al. Central projections of melanopsin-expressing retinal ganglion cells in the mouse. *J Comp Neurol*. 2006;497:326–349.
16. Hattar S, Liao HW, Takao M, Berson DM, Yau KW. Melanopsin-containing retinal ganglion cells: architecture projections, and intrinsic photosensitivity. *Science*. 2002;295:1065–1070.
17. Bissig D, Berkowitz BA. Light-dependent changes in outer retinal water diffusion in rats in vivo. *Mol Vis*. 2012;18:2561.
18. Berkowitz BA, Bissig D, Roberts R. MRI of rod cell compartment-specific function in disease and treatment in-ávivo. *Prog Retin Eye Res*. 2016;51:90–106.
19. Berkowitz BA, Murphy GG, Craft CM, Surmeier DJ, Roberts R. Genetic dissection of horizontal cell inhibitory signaling in mice in complete darkness in vivo. *Invest Ophthalmol Vis Sci*. 2015;56:3132–3139.
20. Berkowitz BA, Roberts R, Bissig D. Light-dependant intraretinal ion regulation by melanopsin in young awake and free moving mice evaluated with manganese-enhanced MRI. *Mol Vis*. 2010;16:1776–1780.
21. Berkowitz BA, Roberts R, Oleske DA, et al. Quantitative mapping of ion channel regulation by visual cycle activity in rodent photoreceptors in vivo. *Invest Ophthalmol Vis Sci*. 2009;50:1880–1885.
22. Berkowitz BA, Roberts R, Goebel DJ, Luan H. Noninvasive and simultaneous imaging of layer-specific retinal functional adaptation by manganese-enhanced MRI. *Invest Ophthalmol Vis Sci*. 2006;47:2668–2674.
23. Berkowitz BA, Bissig D, Patel P, Bhatia A, Roberts R. Acute systemic 11-cis-retinal intervention improves abnormal outer retinal ion channel closure in diabetic mice. *Mol Vis*. 2012;18:372–376.
24. Berkowitz BA, Gradianu M, Bissig D, Kern TS, Roberts R. Retinal ion regulation in a mouse model of diabetic retinopathy: natural history and the effect of Cu/Zn superoxide dismutase overexpression. *Invest Ophthalmol Vis Sci*. 2009;50:2351–2358.
25. Berkowitz BA, Grady EM, Roberts R. Confirming a prediction of the calcium hypothesis of photoreceptor aging in mice. *Neurobiol Aging*. 2014;35:1883–1891.
26. Bissig D, Berkowitz BA. Same-session functional assessment of rat retina and brain with manganese-enhanced MRI. *Neuro Image*. 2011;58:749–760.
27. Cheng H, Nair G, Walker TA, et al. Structural and functional MRI reveals multiple retinal layers. *Proc Natl Acad Sci U S A*. 2006;103:17525–17530.
28. Chen J, Wang Q, Zhang H, et al. In vivo quantification of T1, T2, and apparent diffusion coefficient in the mouse retina at 11.74T. *Magn Reson Med*. 2008;59:731–738.
29. Nickla DL, Totonelly K, Dhillon B. Dopaminergic agonists that result in ocular growth inhibition also elicit transient increases in choroidal thickness in chicks. *Exp Eye Res*. 2010;91:715–720.
30. Fitzgerald MEC, Tolley E, Frase S, et al. Functional and morphological assessment of age-related changes in the choroid and outer retina in pigeons. *Vis Neuro*. 2001;18:299–317.
31. Grunwald JE, Hariprasad SM, DuPont J. Effect of aging on foveolar choroidal circulation. *Arch Ophthalmol*. 1998;116:150–154.
32. Peirson SN, Bovee-Geurts PHM, Lupi D, Jeffery G, DeGrip WJ, Foster RG. Expression of the candidate circadian photopigment melanopsin (Opn4) in the mouse retinal pigment epithelium. *Mol Brain Res*. 2004;123:132–135.
33. Provencio I, Rodriguez IR, Jiang G, Hayes WP, Moreira EF, Rollag MD. A novel human opsin in the inner retina. *J Neurosci*. 2000;20:600–605.
34. Carter-Dawson LD, Lavail MM, Sidman RL. Differential effect of the rd mutation on rods and cones in the mouse retina. *Invest Ophthalmol Vis Sci*. 1978;17:489–498.
35. Semo M, Peirson S, Lupi D, Lucas RJ, Jeffery G, Foster RG. Melanopsin retinal ganglion cells and the maintenance of circadian and pupillary responses to light in aged rodless/coneless (rd/rd cl) mice. *Eur J Neurosci*. 2003;17:1793–1801.
36. Ruan GX, Zhang DQ, Zhou T, Yamazaki S, McMahon DG. Circadian organization of the mammalian retina. *Proc Natl Acad Sci U S A*. 2006;103:9703–9708.

Investigative Ophthalmology & Visual Science